The quarter-wavelength average velocity: a review of some past and recent application developments

V. Poggi, B. Edwards & D. Fäh
Swiss Seismological Service, ETH Zürich, Switzerland

SUMMARY:

In recent years, the large availability of Vs_{30} measurements has imposed this parameter as a standard for seismic site classification of most seismic codes. However, the possibility of using Vs_{30} for ground motion prediction at arbitrary frequencies proved highly controversial, especially at relatively long periods. The quarter-wavelength approach was developed to partially overcome this limitation. The method basically consists in computing frequency-dependent average seismic parameters (velocity and density) and the corresponding amplification factors from a given 1D model. The advantage of such a procedure is the possibility of relating the depth over which the average will be computed to a specific wavelength.

In this study we will present a review of some past and present achievements in using quarter-wavelength approaches for the characterization of rock and soft sediment sites, with specific regards to those studies which have been performed for the characterization of the Swiss digital seismic network.

Keywords: Average velocity, Vs30, seismic amplification, attenuation, seismic hazard.

1. THE QUARTER-WAVELENGTH VELOCITY AND SEISMIC IMPEDANCE

The quarter-wavelength approximation was initially proposed by Joyner et al. (1981), and subsequently optimized by Boore (2003) to compute amplification factors for generic rock profiles. The method is based on the estimation of the average seismic parameters (in particular the velocity Vs^{Qwl}) up to a depth $z(f)$ that corresponds to one quarter of the wavelength of interest. For a specific frequency, amplification factors can then be computed as square root of the impedance ratio between average depth and reference. The quarter-wavelength velocity (Vs^{Qwl}), can be obtained for a specific frequency by travel-time averaging over the input profile, through the minimization of:

$$\arg\min_{z(f)} \left\| z(f) - \frac{Vs^{QWL}\big(z(f)\big)}{4f} \right\| \tag{1.1},$$

given that:

$$Vs^{QWL}\big(z(f)\big) = z(f) \left(\int_{0}^{z(f)} \frac{1}{Vs\big(z(f)\big)} \, dz(f) \right)^{-1} \tag{1.2}.$$

This is achieved through a direct search approach over z in order to recursively converge to the solution of the minimization problem.

However, using the quarter-wavelength average velocity alone is not sufficient to characterize the variability of the ground-motion at soft sediment sites. Spectral amplification induced by resonance phenomena is related to the contrast of the seismic impedance at depth. For this reason, we introduce

the concept of quarter-wavelength seismic impedance contrast (IC^{Qwl}). Such an approach gives the possibility of directly relating the seismic velocity contrast with specific spectral ordinates.

In practice, the IC^{Qwl} parameter can be described as the velocity contrast obtained from the ratio between two quarter-wavelength average velocities (Figure 1, Equation 1.3). The top estimate corresponds to the classic travel-time velocity averaged down to a depth (Z_1) corresponding to ¼ of the wavelength of interest λ_1 (classical quarter wavelength depth). The bottom velocity estimate is obtained as the average along the velocity profile from the depth Z_1 to $Z_1 + \lambda_2/4$. λ_2 is related to λ_1 by keeping the considered frequency constant.

$$IC^{Qwl}(f) = \frac{Vs_1^{Qwl}(f, \lambda_1/4)}{Vs_2^{Qwl}(f, \lambda_2/4)} \qquad (1.3).$$

In sedimentary basins with a strong velocity contrast, the IC^{Qwl} curve includes characteristic troughs, directly related to the most significant interfaces at depth. The first trough when moving along the frequency axis of such a curve can be reasonably considered as a good proxy for the fundamental frequency of resonance of the site.
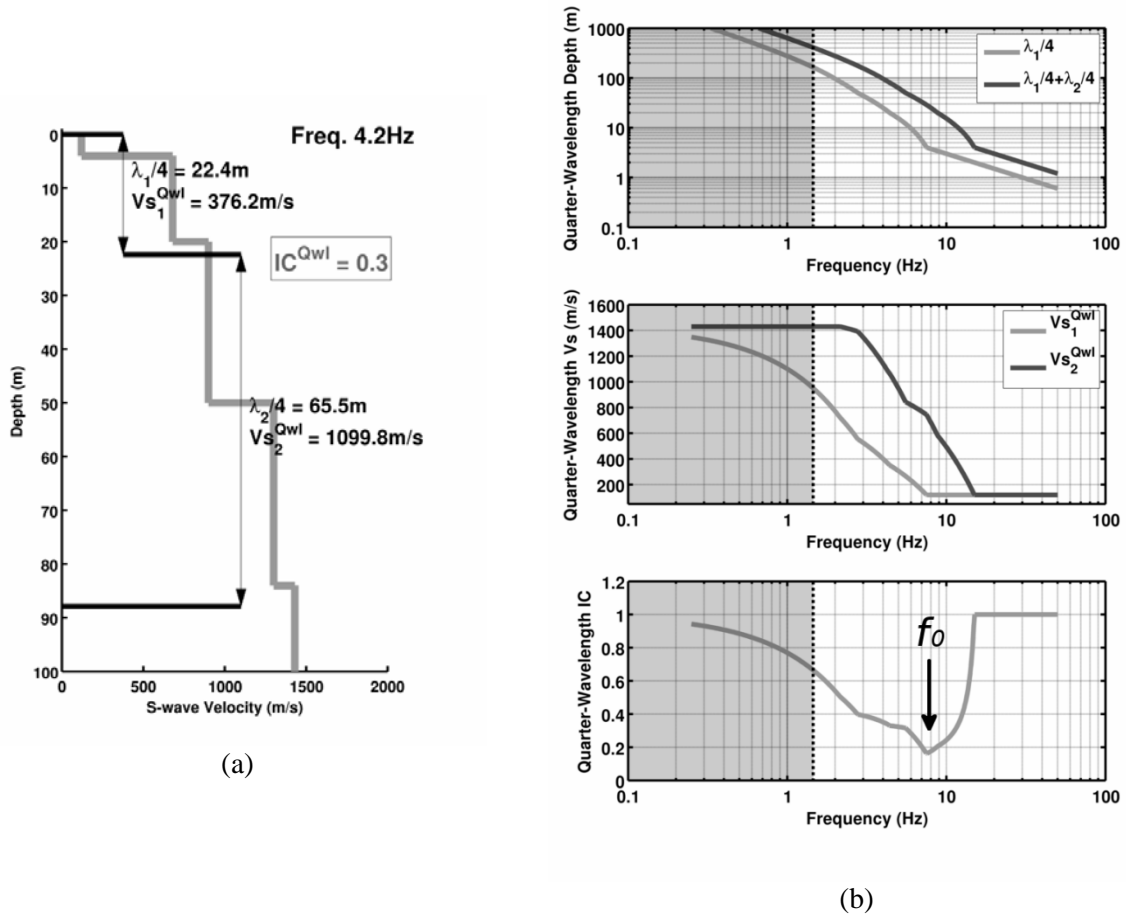

(a)

(b)

Figure 1. Example of quarter-wavelength depth (λ/4), velocity (Vs^{Qwl}) and seismic impedance contrast (IC^{Qwl}) curves (b) of a shear-wave velocity profile (a). The black dashed line defines the frequency region of reliability, where the curves are constrained by the measured velocity profile.
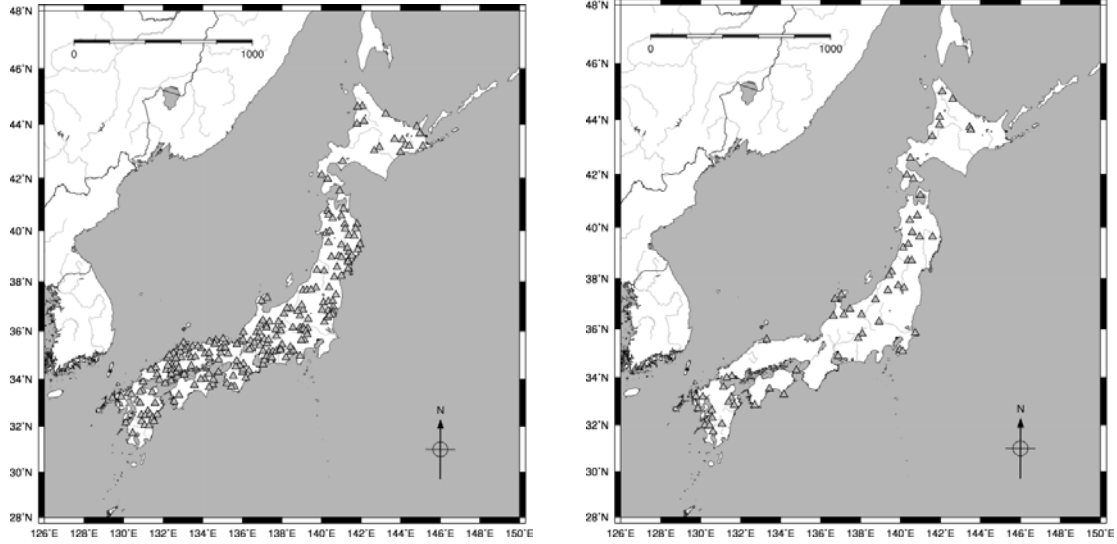
Figure 2. Location of the selected sites of the Japanese KiKNet network. On the left the 220 soft sediment sites, and on the right the 59 stiff-soil and rock sites.

2. THE CALIBRATION DATABASE: THE JAPANESE KIK-NET STRONG-MOTION NETWORK

2.1 Selection Of The Velocity Profiles

Due to the limited extension of the Swiss database (about 100 sites) it was decided to use data from the Japanese KiKNet strong-motion database (Aoi et al., 2004). This gives us the possibility of a more robust statistic on the parameters that will be analyzed in such framework. The KiKNet strong-motion network consists in a total of 689 station locations; for each site a borehole is available, which accommodate two sensor installations, on the top and on the bottom. From the borehole logging, a shear-wave velocity profile was made available at each location by the Japanese National Research Institute for Earth Science and Disaster Prevention (NIED). Unfortunately no uncertainty estimate is available for these profiles. From the whole dataset with 689 sites, a subset of 220 soft sediment sites (Figure 2, left) and 59 stiff-soil to rock sites (Figure 2, right) were manually extracted and analyzed in this study. The sites were selected based on the comparison of the fundamental frequencies of resonance (f_0) directly estimated from the recordings and by indirect modeling methods using the velocity profile. For all the selected profiles, quarter-wavelength velocity and seismic impedance contrast curves were produced.

2.2 Obtaining The Site-Dependent Empirical Amplification Functions

Empirical amplification functions for each site of the Japanese network were derived from spectral modeling (e.g., Edwards et al., 2008; Poggi et al., 2011) of a large number of earthquake events. Using such approach, the transfer function (site term) can be represented as a combination of different terms:

$$T\left(A, f, \kappa\right) = A^{DC}\, a\left(f\right) \mathrm{e}^{\left(-\pi f \kappa\right)} = A^{DC}\, A^{L}\, A^{K} \tag{2.1},$$

where A^{DC} is the average site amplification relative to the _unknown_ reference rock profile (the average amplification over all frequencies), k is the constant, site-related attenuation operator (e.g., Anderson and Hough, 1984) and $a\left(f\right)$ is the frequency dependent site amplification function (e.g. Figure 3).
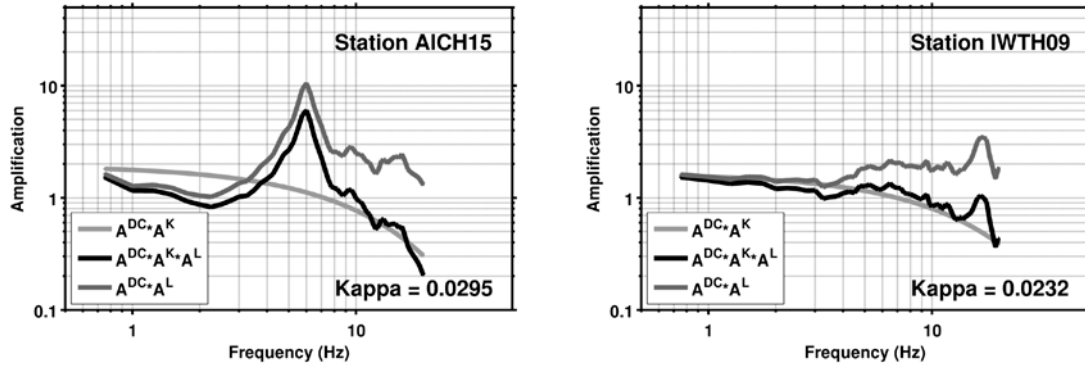
Figure 3. Example of SH-wave amplification functions for a soft sediment site (left) and a rock site (right). Elastic (dark gray) and visco-elastic contributions (black) are presented together for comparison.

3. DEFINING THE ROCK REFERENCE PROFILE FROM QWL-AVERAGE VELOCITIES

A reference velocity profile for Japan can be nevertheless obtained from the comparison of quarter-wavelength average velocities at specific seismic station locations with the corresponding amplification obtained from spectral modeling (Poggi et al., 2011). As such, each average velocity estimates (versus depth) will be uniquely associated to a specific amplification factor at a defined frequency. For the calibration, 59 selected seismic station locations from the Japanese KiKNet network were used. From the ensemble of all measurement locations, amplification versus average velocity relationships (log-log linear correlations) was computed for a set of discrete frequencies between 1 and 8 Hz (e.g. Figure 4).
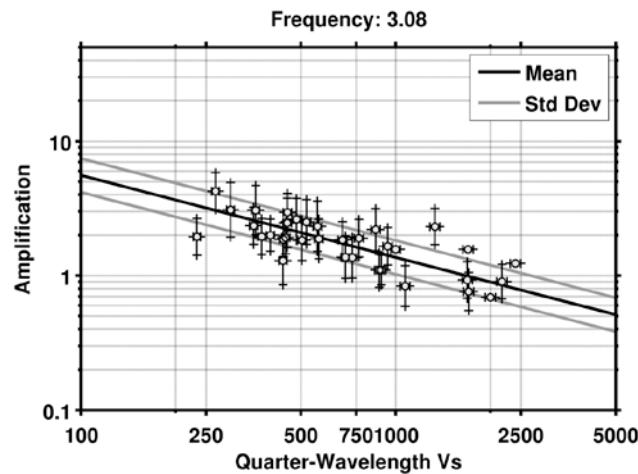

Figure 4. Correlation between quarter-wavelength average velocities and amplification factors from spectral modeling of earthquake spectra. A linear least-squares regression is applied in log-log scale to estimate parameter correlation.
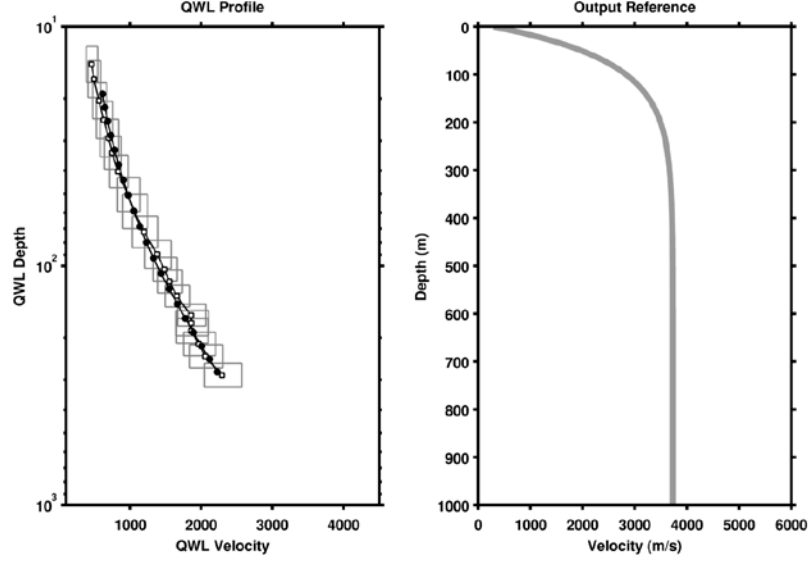
Figure 5. On the left, quarter-wavelength representation of the reference velocity profile obtained from the correlations between quarter-wavelength average velocities and amplification factors. On the right, the inverted reference velocity profile in standard representation.

Then, assuming that the reference profile is defined by a lack of any relative amplification, the expected quarter-wavelength average velocities corresponding to relative "unitary" amplification were extracted and collected from these relations separately. By collecting the average velocity estimates at the different frequencies, a quarter-wavelength representation of the reference velocity profile is therefore established (Figure 5, left). However, for site characterization, a representation of the shear wave velocity profile versus depth is required. This can be subsequently obtained through an inversion procedure (Figure 5, right). This profile represents the reference for the amplification functions, observed or back-computed using the coefficients of the aforementioned correlations at sites with known quarter-wavelength profile.

4. SITE AMPLIFICATION AT SOFT SEDIMENT SITES

For rock sites a clear correlation between the ground motion and quarter-wavelength average velocity of a site exists (Edwards et al, 2011). However, in the case of soft sediment sites, particularly for those with a large contrast of seismic velocity at depth, the influence of a resonance phenomena and the generation of surface waves are important. These will therefore affect the amplification functions, which in this case not only depend on the average velocity estimates from the profile, but also on the impedance contrast (Poggi et al. 2012). This is evident by separating out the different contributions to the total amplification of Equation 2.1: while A^L and A^k are directly related to the velocity variation along the profile (Figure 6) - as it was observed for the rock sites - the local amplification term A^L, which contains the resonance information, will mostly be influenced by the seismic velocity contrast at increasing averaging depths. For this reason, the quarter-wavelength seismic impedance contrast parameter, IC^{QWL}, has been introduced in the correlation with the observed amplification and quarter-wavelength velocity representation (Vs^{Qwl}) of the measured shear-wave velocity profiles (Figure 7):

$$\ln\left(T(f)\right) = \ln\left(A^{DC}A^k\right) + \ln\left(A^L\right) = a \cdot \ln\left(Vs^{QWL}\right) + b \cdot \ln\left(IC^{QWL}\right) + c \qquad (4.1).$$

As a result of the correlation analysis, regression coefficients are then provided for a set of discrete frequencies in the range between 0.5 and 20Hz. Extending the correlation in this three-dimensional space is useful in a general way to reconstruct the generic amplification function of any sites with velocity profile of sufficient depth (Figure 8 and 9).
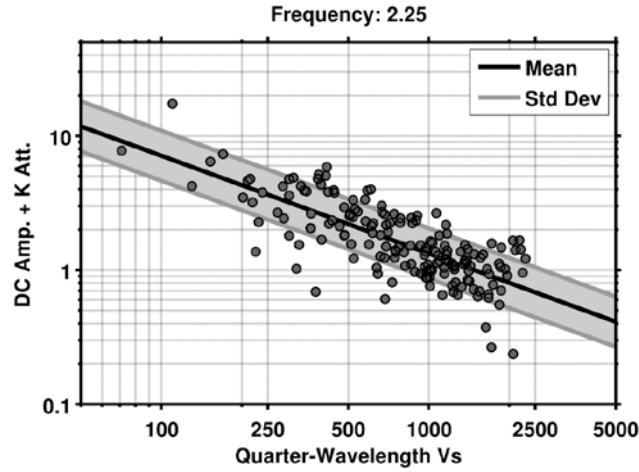
Figure 6. Frequency dependent relation between the damped site term $A^{DC}A^k$ with the quarter-wavelength average velocity at the different sites. Here and example at 2.25Hz.
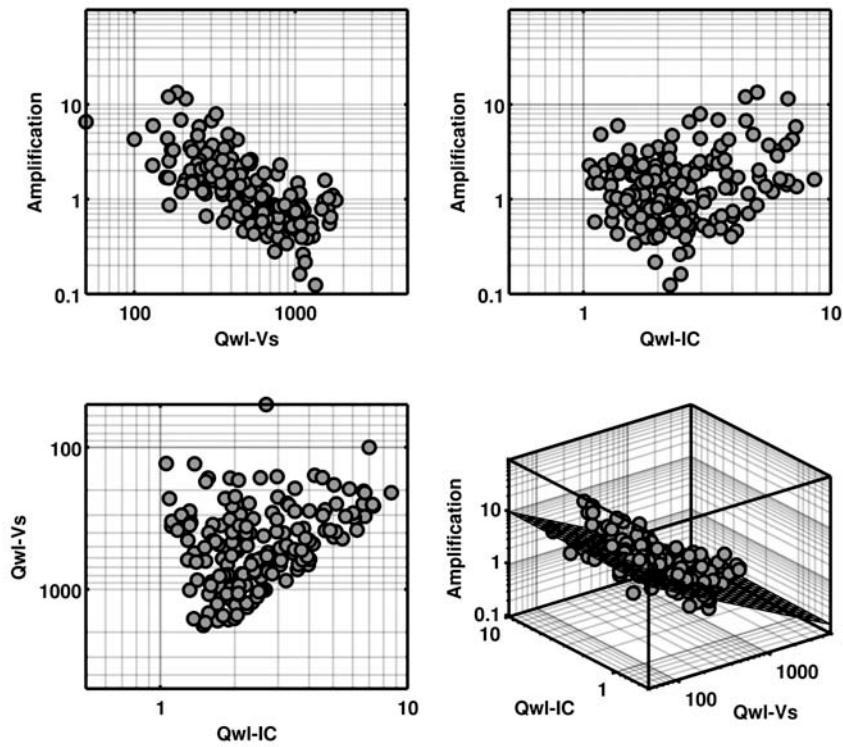

Figure 7. Correlation between the empirical amplification from spectral modeling, the ¼ wavelength-Vs (Vs^{Qwl}) and the ¼ wavelength-IC (IC^{Qwl}) parameters. For the regression, the 220 selected sites of the Japanese network were used. Each dot corresponds to one site. The plots are for a frequency of 3.5Hz.
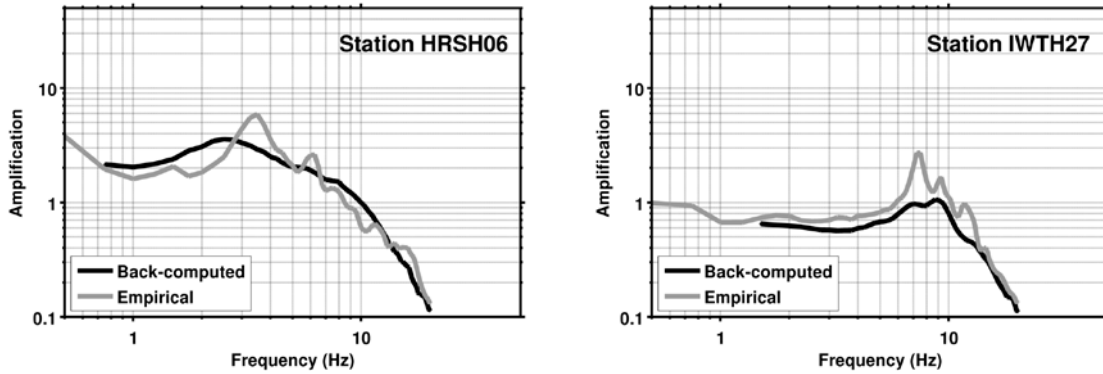
Figure 8. Comparison between empirical and back-computed amplification functions at two example KiK-Net test sites using the coefficients from the frequency dependent correlations.
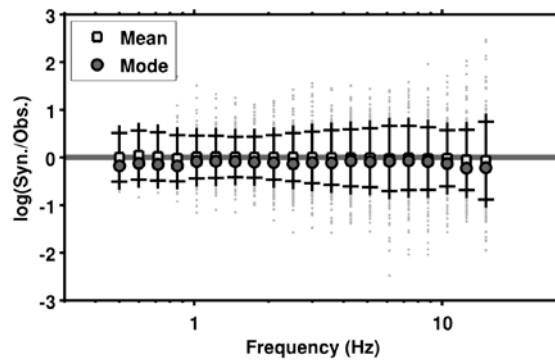

Figure 9. Distribution of the residuals between observed (empirical) and computed amplification functions over the analyzed frequency range (0.5-20Hz).
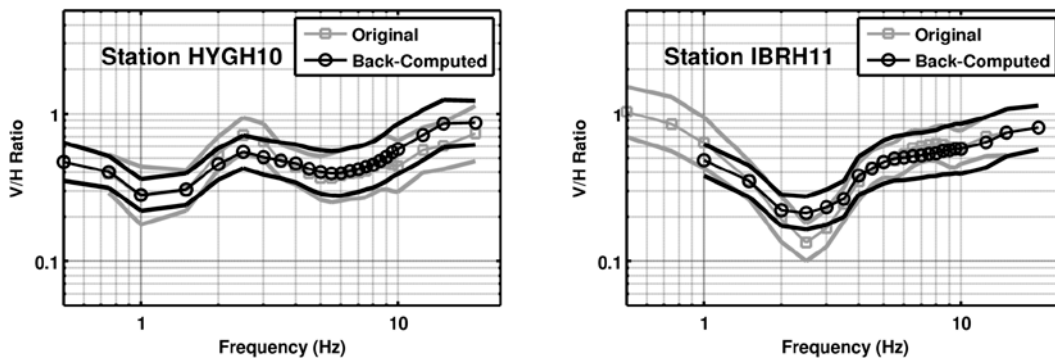

Figure 10. Back-computation of the *V/H* response spectral ratio at four KiK-Net stations using the coefficients from the frequency dependent correlations. Mean and mean +/- standard deviation are given.

A similar type of correlation with the quarter-wavelength parameters exists not only for amplification functions, but can also be established for the vertical-over-horizontal ratios of the 5% damped response spectra at soft sediment sites (Poggi et al. 2012), which in this case are also strongly affected by the presence of local resonance phenomena. As well, the predictive equations can be used to reconstruct the V/H ratio of the ground motion at any sites with known shear-wave velocity profile (Figure 10).
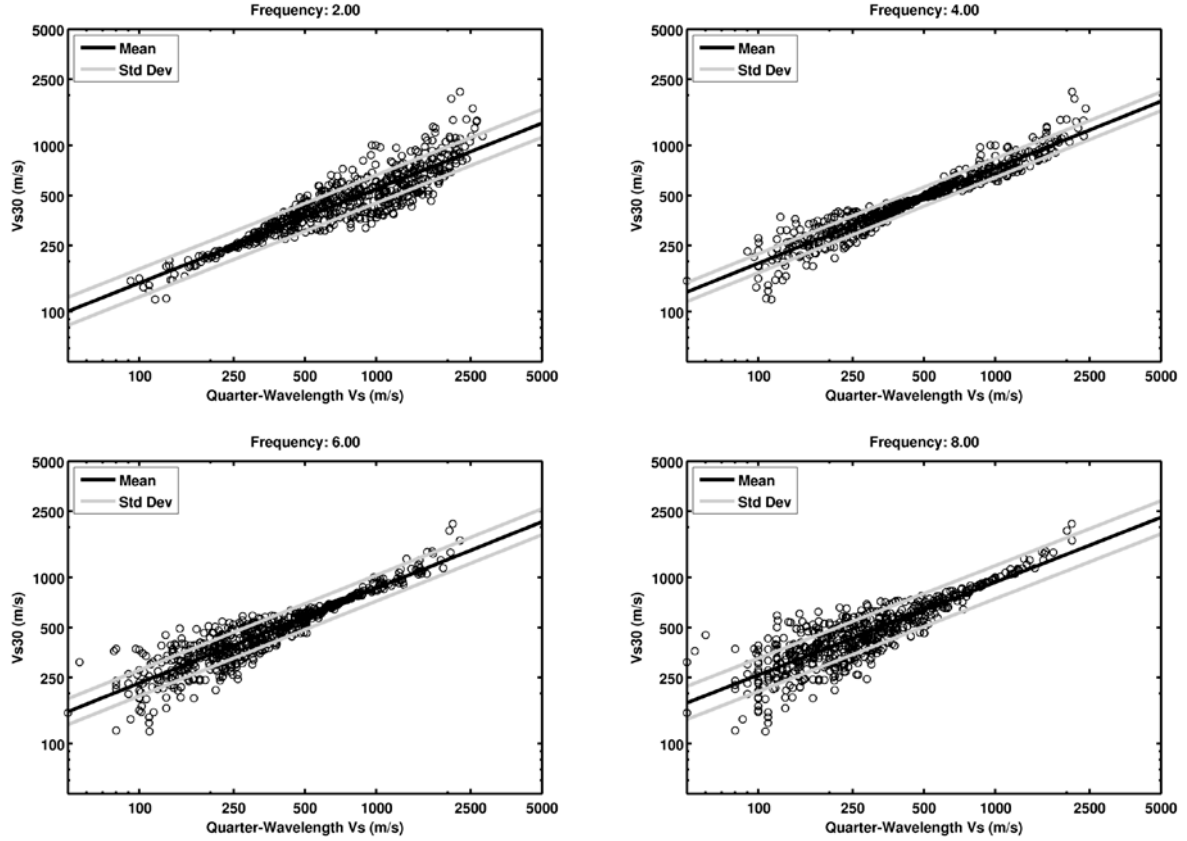
Figure 11. Example of correlation between Vs_{30} and Vs^{Qwl} at four discrete frequencies (2, 4, 6 and 8Hz). Each dot represents a station.

5. DOES A RELATION BETWEEN QWL-VS AND VS30 EXIST?

We now empirically demonstrate that a correlation between Vs_{30} and quarter-wavelength average shear-wave velocity at discrete spectral ordinates exists. For each of the 660 station locations of the Japanese KiKNet network, average Vs_{30} were calculated together with the Vs^{Qwl} velocities from the available velocity profiles. Average velocity estimates have then been compared in the frequency range 1-10Hz, with a 0.5Hz step (e.g. Figure 11). For each analyzed frequency, a clear correlation is noticeable, which appears to be linear in the log-log axis domain. It is therefore possible to establish a log-linear regression in the form:

$$Vs_{30} = \left(Vs^{Qwl}(f) \right)^{a(f)} e^{b(f)}$$

(5.1).

As expected, data distribution is not uniform. For each frequency it is evident a specific velocity value (in both variables) where the spreading of data with respect to the average line is minimum. For example, at 4Hz is at about 500m/s. This corresponds to the point where, at this frequency, the Vs^{Qwl} estimate matches Vs_{30}, and consequently the quarter-wavelength averaging depth (z^{Qwl}) is equal to 30m at the analyzed frequency, according to the relation:

$$z^{Qwl} = \frac{Vs^{Qwl}(f)}{4f} = \frac{Vs_{30}}{4f} = 30m$$

(5.2).

More generally, at high frequencies, the scatter of the data distribution increases at low velocities, while the situation reverses at low frequencies. This is relevant in the sense that the prediction will generally work better for rock sites at relatively high frequency.

By comparing the regression results between the analyzed frequencies a clear trend is evident (Figure 12). While the regression slope is practically unmodified, the intercept progressively increases with increasing frequencies. Therefore, under the assumption of stability of such behavior, it is possible to establish a functional relation which can be used to predict the regression coefficients at frequencies not directly constrained by the available data. An additional advantage of such relation is to minimize the scatter of regression results at the frequency limits of investigation, where the spreading of data might be important.

As further simplification, it must be noticed that the slopes values do not change significantly at the analyzed frequencies. By averaging, therefore, we can impose a unique constant slope value of *0.5636*. The relation simplifies then in:

$$Vs_{30} = \left(Vs^{Qwl}\right)^{0.5636} e^{0.0859f + 2.275}$$

(5.3),

or, conversely, as function of Vs_{30}:

$$Vs^{Qwl} = \left(Vs_{30} \ e^{-(0.0859f + 2.275)}\right)^{1/0.5636}$$

(5.4),

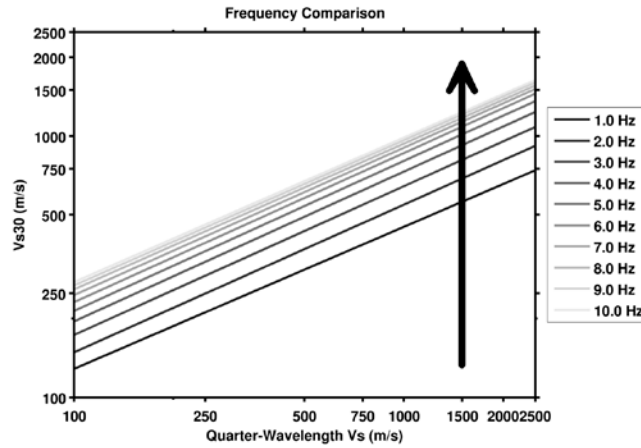which is useful to extrapolate the Vs^{Qwl} velocities at any frequency, given a specific Vs_{30} estimate.

Figure 12. Comparison between all the Vs_{30}-Vs^{Qwl} regressions preformed in the frequency range 1-10Hz. While regression slopes are basically constant, intercepts smoothly increases with increasing frequencies.

6. CONCLUSIONS

In this paper we provided some examples of using the quarter-wavelength approach to assess average ground parameters for seismic site response analysis. Such method demonstrates to be advantageous for the characterization of the ground motion at the surface, which is necessary for GMPEs and site-dependent seismic hazard analysis. In particular, the quarter-wavelength average velocity show up to have the potential to be used as direct proxy for the local site characterization, as it physically relates the resolution on ground parameters with the characteristics of the propagating wave-field at the discrete frequencies. Complementary, computation of the IC^{Qwl} parameter demonstrate to be a powerful tool to assess the influence of resonance phenomena in soft sediment sites. In the paper it is also shown that an empirical relation between Vs_{30} and QWL average-velocity exists. This is of particular relevance, since it provides an additional evidence to understand the reason why Vs_{30} generally works as first order proxy for site amplification.

It has to be noticed, however, that from the engineering point of view the quarter-wavelength parameters are unquestionably of more difficult implementation to the end user, if compared to the classical Vs_{30} estimator. Moreover, the method requires a reliable and sufficiently accurate assessment of the S-wave velocity structure down to a sufficient depth, which is in practice not always available due to the high costs of most common investigation approaches. Nevertheless, the quantity and quality of information carried by this approach is considerable and justifies the additional effort. A clear demonstration of its advantage stays in the accuracy in predicting surface ground motion parameters, such as the amplification factors and horizontal-to-vertical polarization.

For the future, we plan to further investigate the capability and limitations of the quarter-wavelength method, with special regards to anelastic attenuation and to the definition of the uncertainties of the soil amplification factors, which is a key issue in probabilistic hazard assessment.

REFERENCES

Anderson, J. G., and Hough, S. E. (1984). A model for the shape of the Fourier amplitude spectrum of acceleration at high frequencies, *Bull., Seismol., Soc. Am.*, **74**, 1969-1993.

Aoi, S., T. Kunugi and Fujiwara, H. (2004). Strong-Motion Seismograph Network Operated by NIED: K-Net and KiK-Net, *Journal of Japan Association for Earthquake Engineering*, **4:3** (Special Issue).

Boore, D., (2003). Simulation of ground motion using the stochastic method. *Pure and applied Geophysics*, **160:3-4**, 635–676.

BSSC, Building Seismic Safety Council (2003). The 2003 NEHRP Recommended provisions for new buildings and other structures. Part 1: provisions (FEMA 450), www. bssconline.org.

CEN, European Committee for Standardization (2004). Eurocode 8: design of structures for earthquake resistance - part 1: general rules, seismic actions and rules for buildings. Bruxelles.

Edwards, B., A. Rietbrock, J. J. Bommer, and Baptie, B. (2008). The Acquisition of Source, Path and Site Effects from Micro-earthquake Recordings using Q Tomography: Application to the UK, *Bull. Seismol. Soc. Am.*, **98**, 1915–1935.

Edwards, B., V. Poggi and Fäh, D. (2011). A Predictive Equation for the Vertical to Horizontal Ratio of Ground-Motion at Rock Sites based on Shear Wave Velocity Profiles: Application to Japan and Switzerland. *Bull. Seism. Soc. Am.*, **101:6**, 2998-3019.

Joyner, W. B., R. E. Warrick, and Fumal, T. E. (1981). The effect of Quaternary alluvium on strong ground motion in the Coyote Lake, California, earthquake of 1979, *Bull. Seism. Soc. Am,.* **71**, 1333-1349.

Poggi, V., B. Edwards, and Fäh., D. (2011).Derivation of a Reference Shear-Wave Velocity Model from Empirical Site Amplification, *Bull. Seis. Soc. Am.*, **101**, 258-274.

Poggi, V., B. Edwards, and D. Fäh., (2012). Characterizing the vertical to horizontal ratio of ground-motion at soft sediment sites, *Submitted to Bull. Seis. Soc. Am.*

Renault, P., S. Heuberger and Abrahamson, N.A. (2010), PEGASOS Refinement Project: An improved PSHA for Swiss nuclear power plants, in *proceedings of 14ECEE - European Conference of Earthquake Engineering*, Ohrid, Republic of Macedonia, Paper ID 991.